

# Five-hour Half-life of Mouse Liver Gap-Junction Protein

REGIS F. FALLON and DANIEL A. GOODENOUGH

*Department of Anatomy, Harvard Medical School, Boston, Massachusetts 02115*

**ABSTRACT** The half-life of a gap-junction polypeptide band migrating at 21,000  $M_r$  on SDS polyacrylamide gels isolated from mouse liver is measured to be 5 h. Two low-molecular weight bands, probably related to the 21,000  $M_r$  material by proteolysis, have measured half-lives of 4.6 and 5.2 h. Gap junctions are labeled in vivo using the  $^{14}\text{C}$ -bicarbonate labeling procedure, followed by quantitative fluorography.

Intercellular communication, which is mediated by gap junctions, can be regulated in most tissue systems by factors such as a rise in intracellular calcium and a decrease in intracellular pH (32, 37, 38). The time-course of regulation, both the uncoupling and coupling of communication, varies over time-scales ranging from seconds (27) and minutes (5, 21, 22, 38) at one extreme to tens of hours (9) at another. These differences in time-scale are partly the result of differences both in the experimental protocols and in the cells studied. Structurally, the regulation of intercellular communication could occur either at the level of the connexon (subunit) of the gap junction, involving the closing and opening of intraconnexon channels (29, 39), or by disassembly, followed by *de novo* assembly of new connexons.

If the gap junction proteins have half-lives longer than the time necessary for cells to couple or uncouple, this would suggest that the uncoupling event is a reversible phenomenon at the level of the connexon itself. If the protein turnover is faster than the time required to uncouple and recouple cells, this would allow for disassembly and *de novo* connexon assembly to play a role in the regulation process.

Data on the half-lives of gap junction proteins are limited. Gurd and Evans (17) used a double-label isotope technique to estimate the relative turnover time of a "sarcosine-resistant fraction" from rat liver plasma membranes, which contained isolated gap junctions. Turnover was reported to be extremely slow, compared to other cellular proteins. However, as is suggested by the enrichment for glycine in the amino acid analyses of these authors (6), the sarcosine-resistant fraction is heavily contaminated with collagen, an extracellular protein which turns over very slowly. In contrast, Yancey et al. (41) reported a 3-h time-point for peak incorporation of pulse-injected [ $^{35}\text{S}$ ]methionine into peptides at 10,000  $M_r$ , derived from isolated rat liver gap junctions.

A difficulty in measuring the half-lives of proteins using conventional pulse-chase techniques with single isotopes is centered on the multiple reutilization of the amino acids, thus giving longer apparent half-lives (11). The [ $^{14}\text{C}$ ]bicarbonate-

labeling technique (34, 35) offers a method to fix [ $^{14}\text{C}$ ]carbonate into the tricarboxylic acid and urea cycles and thus label intracellular pools of arginine, aspartate, and glutamate in the liver. These amino acids, when released from proteins due to protein catabolism, are rapidly transaminated in the liver, releasing  $^{14}\text{CO}_2$  into a large, cold  $\text{CO}_2$  pool. Hence, [ $^{14}\text{C}$ ]carbonate label shows extremely low reutilization (11, 12) and is the isotope of choice for studying degradation of liver proteins (35). Therefore, we have used the [ $^{14}\text{C}$ ]bicarbonate-labeling procedure, followed by the isolation of an enriched gap-junction preparation. By combining sodium dodecyl sulfate (SDS) polyacrylamide gel electrophoresis (PAGE) with quantitative fluorography of the gels, we have determined the half-lives from the specific activities of the principal bands in the enriched junction preparation.

Polypeptides in isolated gap junctions from liver have been reported to have a wide variety of molecular weights. This heterogeneity is partly due to proteolysis, both endogenous and exogenous, and to the strong tendency for gap-junction polypeptides to aggregate in SDS (8, 19, 20, 30). Mouse liver gap junctions have principal polypeptides at 26,000 and 21,000  $M_r$ , which may be related to each other by proteolysis (16, 19). The protocol used in this study isolates a prominent band migrating at 21,000  $M_r$ ; it is not known how many polypeptides migrate in this 21,000  $M_r$  band. It is demonstrated that the gap-junction polypeptide(s) migrating in this band have an average half-life of 5 h.

## MATERIALS AND METHODS

All reagents were purchased from Sigma Chemical Co., St. Louis, Mo. unless stated otherwise.  $\text{NaH}^{14}\text{CO}_3$  (2–10 mCi/mmol) was purchased from New England Nuclear, Boston, Mass. White mice from Charles River Breeding Laboratory (Wilmington, Mass.), weighing 27–30 g, were 49 d old and of either sex. The livers from 20 mice (30–40 g liver) were combined for analysis at each time-point. The animals were sacrificed, four at a time, by cervical dislocation, and the livers dissected immediately and homogenized with a 40-ml VirTis Dounce Homogenizer (VirTis Co., Inc., Gardiner, N.Y.), type B pestle, in 30 ml of ice-cold 1 mM  $\text{NaHCO}_3$ , with 1 mM EGTA,  $10^{-4}$  M phenylmethylsulfonyl fluoride (PMSF) and  $10^{-5}$  M parachloromercuribenzoate (PCMB), pH 8.0, were added to some

trial runs with no apparent change in gel profile. In the routine runs, only 1 mM NaHCO<sub>3</sub> with 1 mM EGTA was used throughout the protocol. The pooled homogenate was diluted to 1 l, allowed to stand on ice for 10 min, and filtered through 32 layers of cheesecloth, and centrifuged at  $1.78 \times 10^5 g_{min}$  in the Beckman JA-10 rotor (Beckman Instruments, Inc., Spinco Div., Palo Alto, Calif.) at 4°C. All centrifugations presented here are calculated from average *g* values of the rotor used. The supernate was discarded, the pellet resuspended in 2 l of buffer and recentrifuged as above for two repeats. Enriched plasma membranes were then prepared using a sucrose step gradient as previously described (13, 16). The membranes were collected and washed ( $1.78 \times 10^5 g_{min}$ , JA-10 rotor), and the pellets resuspended in 20 ml of buffer. While stirring, 20 ml of 1% (w/v) sarkosyl NL-97 (Geigy Industrials, Ardsley, N. Y.) were added at room temperature. Following a spin at  $1.2 \times 10^4 g_{min}$  in the JA-20 rotor at 15°C, the pellet was discarded and the supernate was then centrifuged at  $4.7 \times 10^5 g_{min}$  in the JA-20 rotor at 15°C. The supernate was discarded and the pellet resuspended in 2 ml of 0.1% Brij 58 in buffer [polyoxyethyleneglycol (20) cetylalcohol, ICI America, Inc., Wilmington, Del.] with vigorous pipetting or brief sonication at room temperature. This material was layered on top of a 41%/30% sucrose (wt/vol) step gradient and centrifuged at  $1.2 \times 10^7 g_{min}$  in two buckets of the Beckman SW41 rotor at 15°C. The material at the 41/30 interface was collected, and washed ( $3.0 \times 10^6 g_{min}$ ) at 4°C. The enriched gap junctions may be used at this stage or further purified by repeating the sarkosyl/Brij 58 protocol, substituting 20 ml of 0.5% sodium deoxycholate (DOC) for 20 ml of 1.0% sarkosyl. Yield: 100–200 µg protein/20 animals. Using the zonal rotors (13), this protocol was easily scaled up to 100 animals with average yields of 1 mg protein/run.

### Electron Microscopy

For negative staining, isolated gap junctions were negatively stained with 1% aqueous uranyl formate. For thin sections, pellets of junctions were fixed in 1% glutaraldehyde in 0.1 M sodium cacodylate, pH 7.4, at room temperature for 30 min, postfixed in 2% aqueous OsO<sub>4</sub>, in-block stained with 1% aqueous uranyl acetate, dehydrated with graded ethanols, and embedded in Epon 812. Thin sections were stained with lead citrate.

### Labeling of Junctions

To label junctions, 20 animals were used per time point. 10 mCi of NaH<sup>14</sup>CO<sub>3</sub> (112 mg) were dissolved in 8.6 ml of sterile water, then 0.4 ml of this solution were injected intraperitoneally into each of the 20 mice. The total injection time for all animals averaged  $9.7 \pm 1.4$  min (*N* = 7), the longest time being 11 min. Animals were returned to their cages and allowed to eat and drink *ad libitum* until sacrifice at the appropriate time-point. Time-points selected for this experiment are 3, 6.5, 11, 17.5, 24, and 35 h.

Following isolation of the enriched gap-junction preparation as detailed above, 10% of the final volume of washed junctions was removed and assayed for protein content by the method of Lowry et al. (28), using bovine serum albumin as standard. This step permits a rough estimate of protein concentration such that approximately equal weights of protein can be loaded on each gel lane.

### Gel Electrophoresis and Fluorography

Slab SDS gel electropherograms were run according to the methods of Ornstein (31), Davis (2), and Laemmli (25), using a 5% stacking gel and a 12.5% running gel. Reduced and alkylated standards were run with each gel: myosin, phosphorylase A, bovine serum albumin, catalase, actin, aldolase, carbonic anhydrase, RNase, and cytochrome C. Specimens are dissolved with vigorous pipetting in 1% SDS, 50 mM 2-mercaptoethanol, and 2 M urea, and allowed to stand for 30 min at room temperature, then alkylated according to Dwyer and Blobel (3), although this step produces no observable differences compared to nonalkylated controls. After electrophoresis, gels are stained with Coomassie Brilliant Blue R according to Fairbanks et al. (7).

The stained wet gels (see example, Fig. 5) were then scanned on a Joyce-Loebl scanning microdensitometer (Joyce, Loebl and Co., Inc., Burlington, Mass.), using wedge D-183. Then, the gels were dried and fluorographed according to the methods of Bonner and Laskey (1) and Laskey and Mills (26). Exposure

times were 130 d. The exposed films were developed in Kodak D-19 (see example, Fig. 6) and scanned with a Schoeffel spectrodensitometer, Model SD 3000 (Schoeffel Instrument Corp., Westwood, N. J.) at 550 nm. The areas under the scanned peaks (see example in Fig. 7) were measured with a Zeiss MOP-3 image analyzer (Carl Zeiss, Inc., New York, N. Y.). The specific activity of each peak on the gel was then expressed as the ratio of the area of the fluorograph peak to the area of the Coomassie peak. This specific activity is in arbitrary units but may be used for comparison between time-points and calculation of half-life.

### RESULTS

The isolation protocol, which produces exceptionally high yields of junctions per run (up to 1 mg/150 g liver), has the empirical requirement for EGTA in the homogenization buffer. Addition of EGTA immediately after homogenization results in much lower yields of junctions, for unknown reasons. The resulting enriched preparations are shown in thin-section and negative-stain electron microscopy in Figs. 1–4. Because there is no assay for gap junctions other than morphology, it is important to begin these experiments with highly enriched preparations. As reported by Zampighi and Robertson (42), the addition of the detergent Lubrol (we use here the more purified Brij 58) results in a high degree of crystallinity of the connexons (subunits) of the gap junctions (Fig. 4), with concomitant improvements in the x-ray scattering data (15). The isolated junctions are morphologically highly enriched, with little amorphous material and collagen contaminating the preparation.

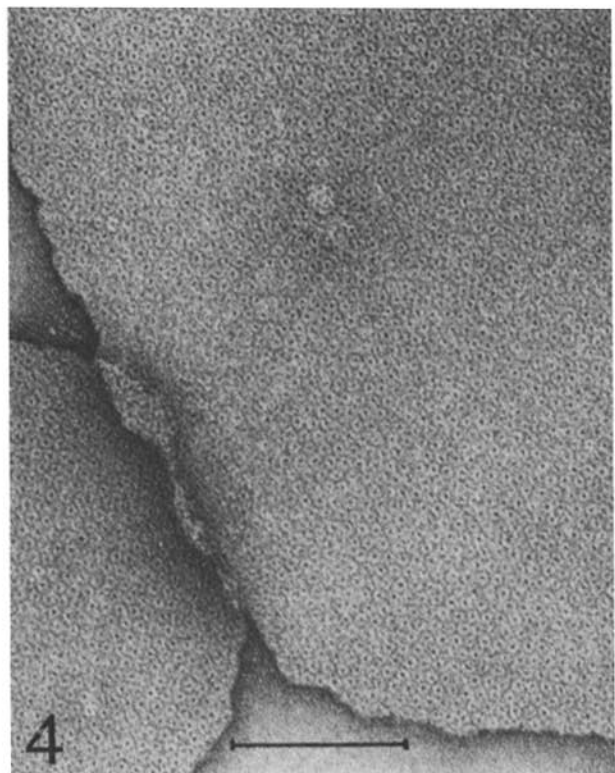
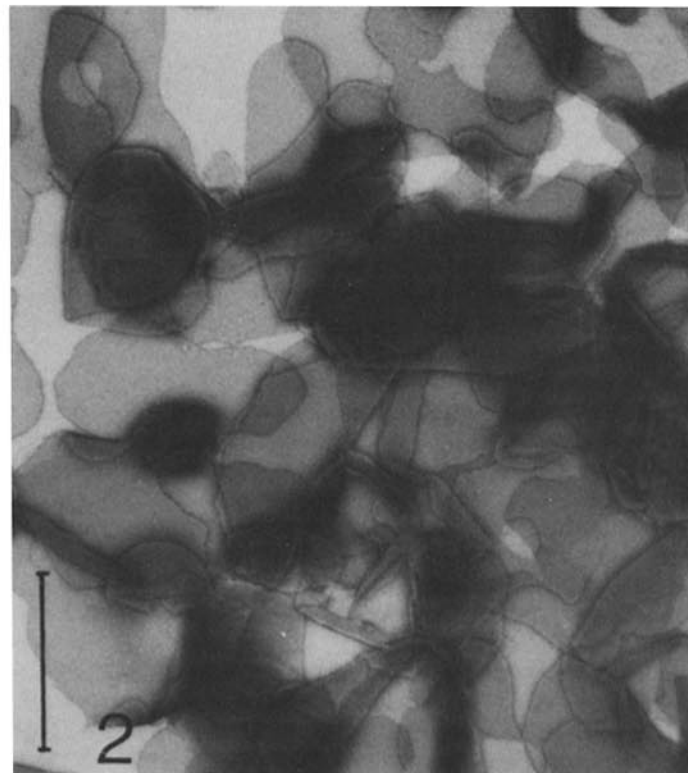
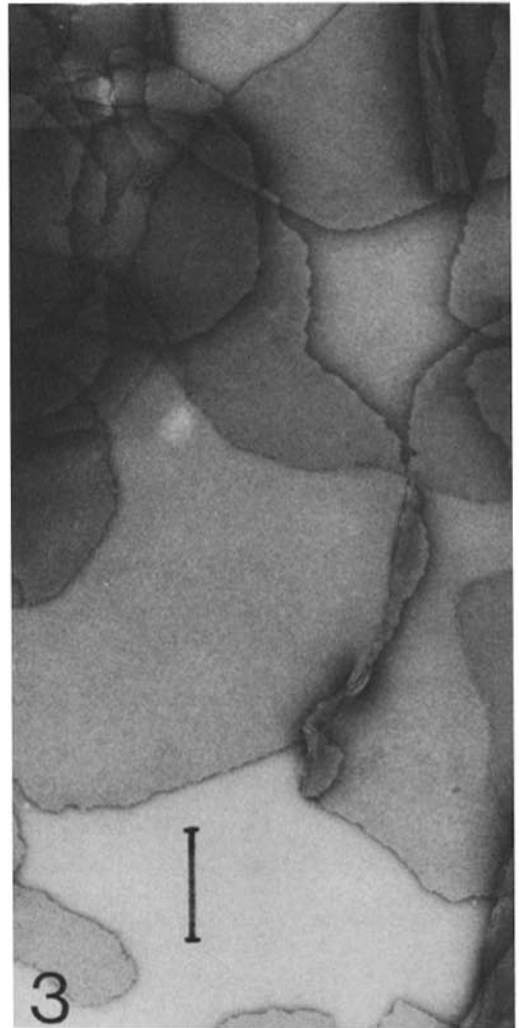
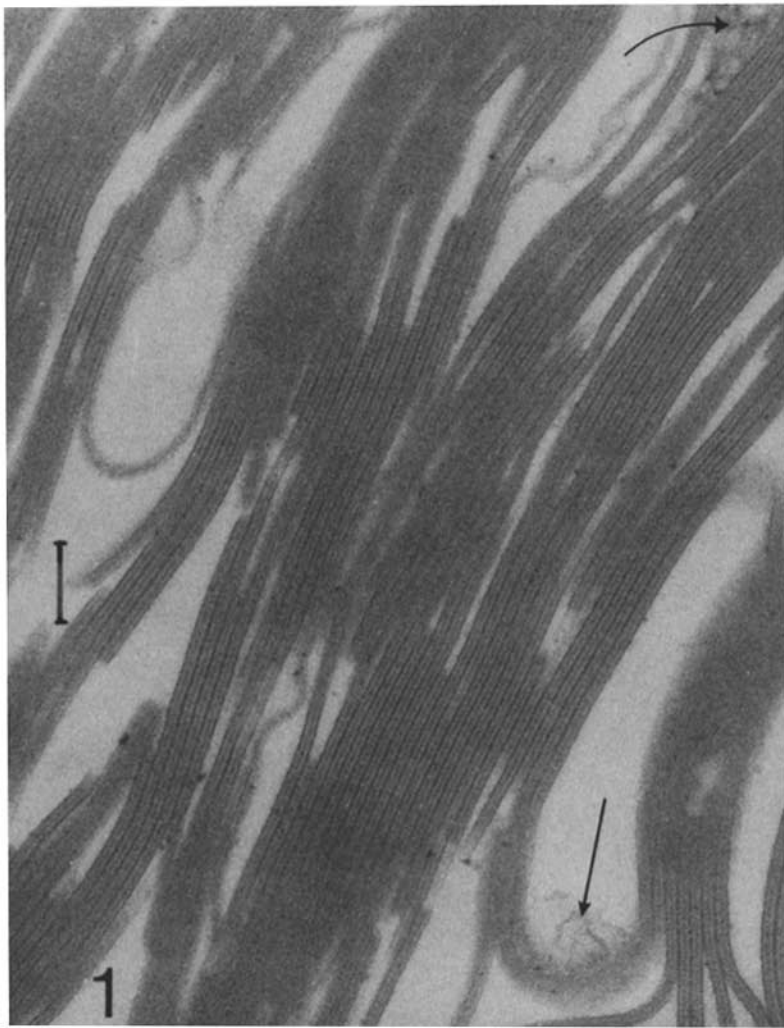
A photograph of an SDS polyacrylamide gel of the isolated gap-junction proteins is shown in Fig. 5. Each lane represents the proteins from a different time-point as indicated on the figure. Each specimen is characterized by a prominent band at 21,000 *M<sub>r</sub>* with variable amounts of additional material migrating at 22,000 and 26,000 *M<sub>r</sub>*. There are one or two broad bands running in the 40,000–45,000 *M<sub>r</sub>* region of the gel, variable from lane to lane, and there are multiple low molecular weight bands in the 10,000–13,000 *M<sub>r</sub>* region of the gel, also varying in number and quantity from lane to lane.

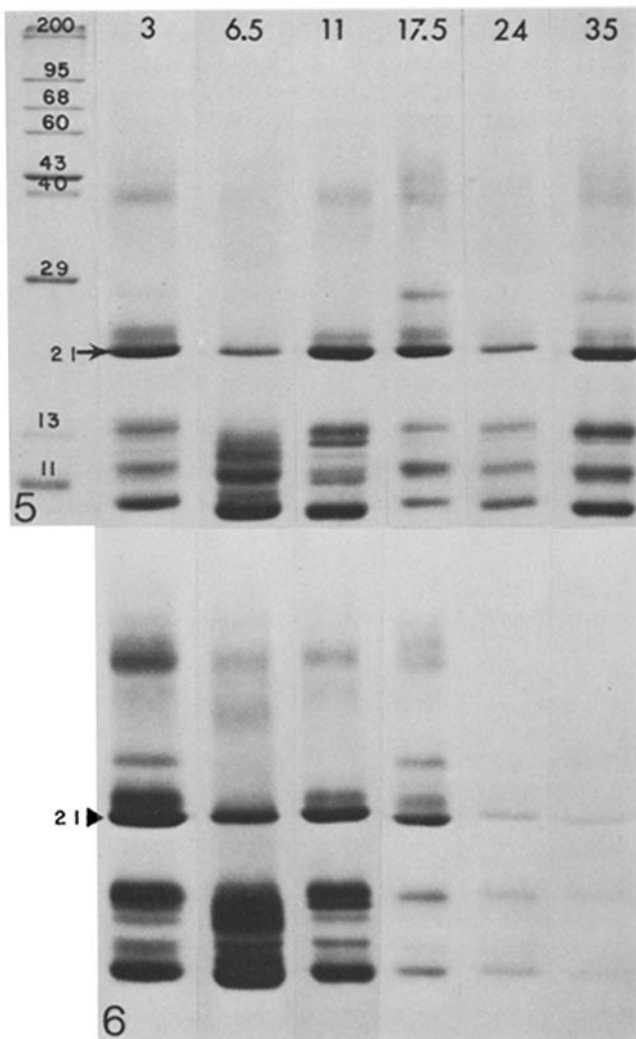
Henderson et al. (19) have analyzed gel profiles of mouse liver gap junctions in detail, and have shown a conversion of the two polypeptides, 26,000 and 21,000 *M<sub>r</sub>*, to low molecular weight polypeptides with exposure to exogenous proteases. These authors also demonstrate that the 26,000 and 21,000 *M<sub>r</sub>* polypeptides can aggregate with heating into polypeptides in the 40,000–50,000 *M<sub>r</sub>* region of the gel, a conclusion supported by peptide-mapping data in rat liver (30). Heat-induced aggregation has also been reported for the lens fiber gap-junction principal polypeptide of 26,000 *M<sub>r</sub>* (40). The 21,000 *M<sub>r</sub>* band (in our liver preparations) shows a similar tendency for heat-induced aggregation (data not shown). Some of the low molecular weight material in the 10,000–13,000 *M<sub>r</sub>* region of the gel may be proteolysis products of the 21,000 and 26,000 *M<sub>r</sub>* peptides, as suggested by Henderson et al. (19) and by peptide-mapping studies (30, 41). Thus, the relationship between the various bands seen on the SDS electropherograms and the proteins within the gap junction is complex.

For our degradation studies, we determine a specific activity

FIGURE 1 An electron micrograph of a thin section of a high-speed pellet of the enriched mouse liver gap junctions showing dense accumulations of the hepatolaminar intercellular junctions often aggregated into myelinlike stacks. Amorphous contamination (arrows) and curved junctions interfere with more extensive stacking. Bar, 100 nm.

FIGURES 2–4 Negatively stained with uranyl salts, the enriched gap junctions appear in electron micrographs as irregularly shaped plates, but in some runs appearing more vesicular. Folded edges of the junction (Fig. 3) display the characteristic double membrane profile, and higher magnification (Fig. 4) reveals the hexagonal lattice of connexons. The high order of the crystalline lattice may be seen by viewing Fig. 4 at an oblique angle along one of the (1,0) lattice lines. Bars: Fig. 2, 1 µm; Fig. 3, 250 nm; Fig. 4, 100 nm.





FIGURES 5-6 These figures show a photograph of the Coomassie Blue-stained gel (Fig. 5) and the fluorogram of the same gel (Fig. 6). The molecular weights (in kilodaltons) of the reduced and alkylated standards are shown in lane 1 of Fig. 5. The time point of each specimen is indicated at the top of each lane in Fig. 5; the fluorogram of that time-point is mounted directly beneath in Fig. 6.

for individual protein bands by taking the ratio of the density of the fluorograph peak to the density of the Coomassie peak. In control experiments with a serially diluted single sample, the Coomassie staining of the 21,000  $M_r$  band is linear on a single slab gel over the range of loading used in this study (data not shown). Due to the small size of the specimens and the uneven distribution of protein mass in the gel bands between different time-points, we have not attempted to put this specific activity on an absolute scale.

Fig. 6 shows the fluorograph of the Coomassie-stained gel in Fig. 5. The fluorograph of each time-point is mounted directly beneath its Coomassie-stained counterpart. The data shown here are from a single slab gel; lanes have been cut and remounted to present them in their chronological sequence.

Fig. 7 shows an example of the comparative densitometry of the density of Coomassie staining (Fig. 7B) vs. the density of fluorograph (Fig. 7A). These tracings were taken from the 17.5-h time-point, and are representative of the data used for estimation of the areas under the peaks with the MOP-3.

Fig. 8 shows a graph of the specific activity in arbitrary units of the 21,000  $M_r$  band vs. time. The maximum labeling occurs at the 6.5-h time-point, then the label is lost with exponential

decay kinetics up to the 35-h time-point. Error bars are not included on this figure because the experiment was performed only once, but it should be noted that each data point represents the junctions from 20 separate animals run up in parallel. The inset in Fig. 8 shows a plot of the natural logarithm of the specific activity vs. time, using data from the decay portion of the curve in Fig. 8. The line through the data was calculated by linear regression giving the  $y$ -intercept (3.2) and slope ( $-0.139 \text{ h}^{-1}$ ). This slope is the decay constant ( $k$ ) in the relationship  $A_t = A_0 e^{-kt}$ , where  $A_t$  is the specific activity at time  $t$  and  $A_0$  the initial radioactivity. The half-life of the 21,000  $M_r$  band is thus  $\ln 2 / 0.139 = 5 \text{ h}$ . The coefficient of determination for these data is 0.98. The decay kinetics thus appear to fit a first-order exponential, expected from a single peptide species, and not the multiexponential data expected for mixed proteins with different half-lives (10).

The kinetics of turnover of the two major labeled low molecular weight bands were also measured. These bands are labeled 1 and 2 on Fig. 7A, and they have calculated half-lives of 4.6 and 5.2 h, respectively. The decay curves also fit simple exponentials as with the 21,000  $M_r$  band. Because these peptides turn over with approximately the same half-life as the 21,000  $M_r$  band, this supports the suggestion that they may be proteolysis products of higher molecular weight precursors, as reviewed above. If these low molecular weight peptides are indeed proteolysis products of the 21,000  $M_r$  band, then the differences in calculated half-lives provide an estimate of the experimental error.

## DISCUSSION

In this study, we have measured the turnover of principal polypeptide bands visualized in SDS polyacrylamide gels of

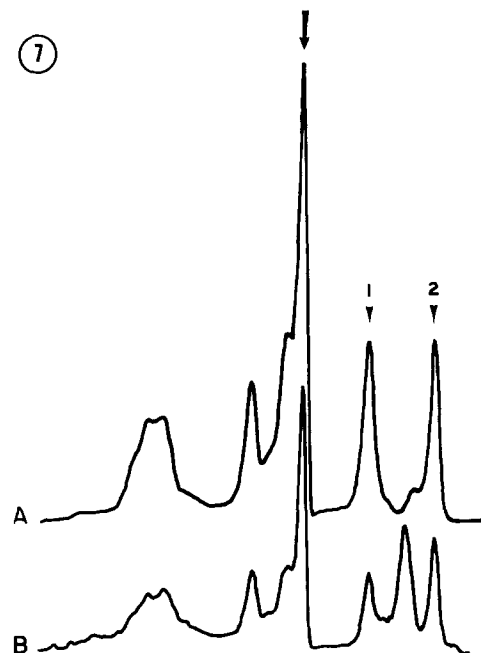


FIGURE 7 This figure compares a densitometric tracing of the 17.5-h lane of the Coomassie Blue-stained gel (B) with a densitometric tracing of the 17.5-h lane of the fluorograph (A). Trace A was made directly from the exposed and developed fluorograph; trace B made directly from the wet, Coomassie Blue-stained gel. The radioactivity closely follows the peaks in Coomassie Blue staining. The 21,000  $M_r$  band is indicated by the arrow. The low molecular weight peptides, whose half-lives are measured, are indicated at 1 and 2.

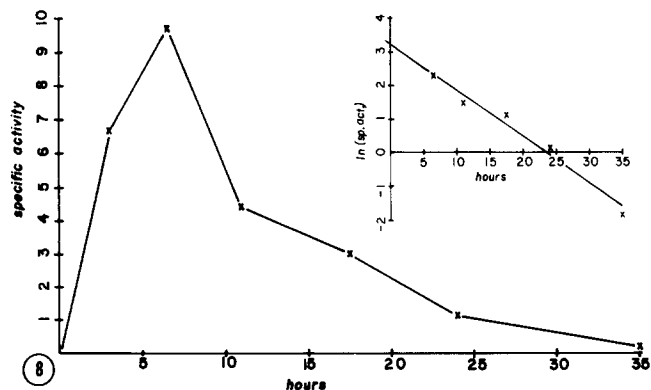


FIGURE 8 This graph plots the specific activity of the 21,000  $M_r$  band, as a function of time following a pulse of  $\text{NaH}^{14}\text{CO}_3$ . The specific activity is expressed in arbitrary units of fluorograph density/Coomassie Blue density. The inset graphs the natural log of the specific activities of the decay portion of the curve in Fig. 8 as a function of time. The line through the points was calculated by linear regression. The slope of this line is the decay constant used to calculate the half-life. The coefficient of determination ( $R^2$ ) is 0.98.

enriched gap-junction preparations. A half-life of the principal SDS PAGE band at 21,000  $M_r$  has been measured at 5 h. This half-life is significantly faster than that measured previously by Gurd and Evans (17), presumably due to inclusion of collagen in the "sarcosine resistant fraction" used by these authors.

In comparison to other plasma membrane proteins from mouse or rat liver, the gap-junction peptide(s) has a strikingly rapid half-life. Average rates of degradation for liver proteins have been estimated with [ $^{14}\text{C}$ ]carbonate labeling to be ~40 h in both the mouse (34) and the rat (10). Sialoglycoproteins in the plasma membrane of rat liver and Morris hepatoma 7777 cells are degraded with half-lives of 23–25 h (18). A major glycoprotein in the plasma membrane of rat liver cells has a half-life of 70–78 h, whereas the oligosaccharide moiety has a shorter half-life of 12–33 h (24). Elovson (4) has shown that two different glycoproteins from the plasma membrane of rat hepatocytes are degraded with distinct half-lives of 24 and 120 h. The asialoglycoprotein-binding protein in hepatocyte plasma membranes has a half-life of 88 h (36).

There are several assumptions underlying this study which must be explicitly pointed out. First, the fractionation protocol isolates at best only 10% of the total gap-junction membrane in the mouse liver (16). It is assumed, therefore, that the same representative fraction is isolated at each time-point. Because 20 animals are used per time-point, and an identical protocol was used on animals allowed to feed *ad libitum* for 24 h under controlled conditions before experimentation, there is no obvious reason to suspect any systematic error introduced by selecting only a fraction of the total junctional surface area.

With regard to the 10% yield, however, an additional point can be made. It is becoming apparent that gap junctions are a class of intercellular interactions, because the junctions isolated from lens fibers (14, 30) and from myocardium (23) show differences in their polypeptide composition compared to each other and to liver junctions. It has also been demonstrated that there are differences in the regulatory properties between chick embryo lens cells joined by embryonic vs. lens fiber specific gap junctions (33). It is likely that the half-lives of these different junctions vary widely, because the lens junctions probably do not turn over at all (14). It is not known whether

liver cells also express "lens fiber" or "myocardial" gap junctions; these would not be expected to survive the treatment with 0.5% sarkosyl used in this protocol. Thus, it is important to recognize that this study measures turnover of liver gap junctions with the 21,000  $M_r$  peptide(s) but that there may be other classes of gap junctions between the hepatocytes which have different half-lives. Additionally, due to this possible heterogeneity of gap junctions in different tissues, the half-life reported here is valid only for mouse liver gap junctions with the 21,000  $M_r$  peptide(s); turnover times for gap junctions in other tissues must be determined on a case-by-case basis.

The data presented here are the result of a single series of experiments to determine the specific activity of junction proteins with time. Due to the high expense of label, multiple repeats have not been performed. A pilot experiment was done, however, to determine the time frame for maximum label incorporation into the junctions. Specific activity in this pilot experiment was measured by dividing samples in half, then measuring protein concentration by the method of Lowry et al. (28) and the total radioactivity by scintillation (data not shown). Whereas these data are not adequate for half-life calculations, we nonetheless found a peak of incorporation at 7 h, supporting the data presented here.

Measurement of the specific activity of two low molecular weight bands on the gels reveals that they have half-lives similar to that of the 21,000  $M_r$  material, and are probably related by proteolysis, as suggested by Henderson et al. (19). This relationship is also suggested by the peptide-map studies of Nicholson et al. (30).

In general, proteins that have important regulatory roles (such as enzymes that catalyze rate-limiting steps in metabolic pathways) tend to have short half-lives (12). This rapid turnover allows concentrations of these proteins to change especially rapidly in response to changing physiological demands. The reason for rapid turnover of mouse liver gap-junction protein is unknown. Because the gap-junction proteins may be proteolyzed in the membrane *in vivo*, before being internalized and further degraded, this may explain why most liver junction isolation protocols yield material that has been partially proteolyzed, despite efforts to work rapidly and to use protease inhibitors. Consonant with this idea, lens fiber gap junctions, which would not be expected to turn over due to the loss of the cell's protein synthetic machinery, reveal a single 26,000  $M_r$  band with little evidence of proteolysis, except perhaps in cases of senility and cataract. There is little information on the mechanisms or time-course of uncoupling of liver cells. If uncoupling and recoupling are slow, as has been demonstrated in RL cells with  $\text{CO}_2$  (9), rapid turnover may be the mechanism for regulation of communication in liver tissue. That is, gap-junctional communication may be controlled by the liver cell at the level of protein synthesis and degradation, rather than a reversible molecular phenomenon at the level of individual connexons.

The expert technical assistance of Mr. J. S. B. Dick II is gratefully acknowledged. This study would not have been possible without the invaluable discussions, encouragement, and suggestions of Drs. J. Fred Dice and A. L. Goldberg. We are indebted to Drs. Alice Y.-C. Liu and Daniel Branton for the use of their densitometry facilities.

This work was supported by grant GM 18974 from the National Institutes of Health.

Received for publication 9 February 1981, and in revised form 1 April 1981.

## REFERENCES

1. Bonner, W. M., and R. A. Laskey. 1974. A film detection method for tritium-labeled proteins and nucleic acids in polyacrylamide gels. *Eur. J. Biochem.* 46:83-88.
2. Davis, B. J. 1964. Disc electrophoresis. II. Method and application to human serum proteins. *Ann. N. Y. Acad. Sci.* 121:404-427.
3. Dwyer, N., and G. Blobel. 1976. A modified procedure for the isolation of a pore complex-lamina fraction from rat liver nuclei. *J. Cell Biol.* 70:581-591.
4. Elovson, J. 1980. Biogenesis of plasma membrane glycoproteins. Tracer kinetic study of two rat liver plasma membrane glycoproteins *in vivo*. *J. Biol. Chem.* 255:5816-5825.
5. Epstein, M., J. D. Sheridan, and R. G. Johnson. 1977. Formation of low-resistance junctions *in vitro* in the absence of protein synthesis and ATP production. *Exp. Cell Res.* 104:25-30.
6. Evans, W. H., and J. W. Gurd. 1972. Preparation and properties of nexuses and lipid enriched vesicles from mouse liver plasma membranes. *Biochem. J.* 128:691-700.
7. Fairbanks, G., T. L. Steck, and D. F. H. Wallach. 1971. Electrophoretic analysis of the major polypeptides of the human erythrocyte membrane. *Biochemistry.* 10:2606-2617.
8. Finbow, M., S. B. Yancey, R. Johnson, and R. P. Revel. 1980. Independent lines of evidence suggesting a major gap junctional protein with a molecular weight of 26,000. *Proc. Natl. Acad. Sci. U. S. A.* 77:970-974.
9. Flagg-Newton, J., and W. R. Loewenstein. 1979. Experimental depression of junctional membrane permeability in mammalian cell culture. A study with tracer molecules in the 300 to 800 Dalton range. *J. Membr. Biol.* 50:65-100.
10. Gartlick, P. J., J. C. Waterlow, and R. W. Swick. 1976. Measurement of protein turnover in rat liver. Analysis of the complex curve for decay of label in a mixture of proteins. *Biochem. J.* 156:657-663.
11. Goldberg, A. L., and J. F. Dice. 1974. Intracellular protein degradation in mammalian and bacterial cells. *Annu. Rev. Biochem.* 43:835-869.
12. Goldberg, A. L., and A. C. St. John. 1976. Intracellular protein degradation in mammalian and bacterial cells: part 2. *Annu. Rev. Biochem.* 45:747-803.
13. Goodenough, D. A. 1974. Bulk isolation of mouse hepatocyte gap junctions. Characterization of the principal protein, connexin. *J. Cell Biol.* 61:557-563.
14. Goodenough, D. A. 1979. Lens gap junctions: a structural hypothesis for non-regulated low resistance intercellular pathways. *Invest. Ophthalmol.* 18:1104-1122.
15. Goodenough, D. A., D. L. D. Caspar, W. C. Phillips, and L. Makowski. 1978. Preparation and characterization of highly ordered gap junction structure. *J. Cell Biol.* 79 (2, Pt. 2): 223a (abstr.).
16. Goodenough, D. A., and W. Stoerkenius. 1972. The isolation of mouse hepatocyte gap junctions. Preliminary chemical characterization and x-ray diffraction. *J. Cell Biol.* 54: 646-656.
17. Gurd, J. W., and W. H. Evans. 1973. Relative rates of degradation of mouse-liver surface membrane proteins. *Eur. J. Biochem.* 36:273-279.
18. Harms, E., and W. Reutter. 1974. Half-life of N-acetylneuraminic acid in plasma membranes of rat liver and Morris hepatoma. *Cancer Res.* 34:3165-3172.
19. Henderson, D., H. Eibl, and K. Weber. 1979. Structure and biochemistry of mouse hepatic gap junctions. *J. Mol. Biol.* 132:193-218.
20. Hertzberg, E. L., and N. B. Gilula. 1979. Isolation and characterization of gap junctions from rat liver. *J. Biol. Chem.* 254:2138-2147.
21. Ito, S., E. Sato, and W. R. Loewenstein. 1974. Studies on the formation of a permeable cell membrane junction. *J. Membr. Biol.* 19:305-337.
22. Johnson, R., M. Hammer, J. Sheridan, and J. P. Revel. 1974. Gap junction formation between reaggregated Novikoff hepatoma cells. *Proc. Natl. Acad. Sci. U. S. A.* 71:4536-4540.
23. Kensler, R. W., and D. A. Goodenough. 1980. Isolation of mouse myocardial gap junctions. *J. Cell Biol.* 86:755-764.
24. Kreisel, W., B. A. Volk, R. Buchsel, and W. Reutter. 1980. Different half-lives of the carbohydrate and protein moieties of a 110,000-dalton glycoprotein isolated from plasma membranes of rat liver. *Proc. Natl. Acad. Sci. U. S. A.* 77:1828-1831.
25. Laemmli, U. K. 1970. Cleavage of structural proteins during the assembly of the head of bacteriophage T4. *Nature (Lond.)* 227:680-685.
26. Laskey, R. A., and A. D. Mills. 1975. Quantitative film detection of <sup>3</sup>H and <sup>14</sup>C in polyacrylamide gels by fluorography. *Eur. J. Biochem.* 56:335-341.
27. Loewenstein, W. R., Y. Kanno, and S. J. Socolar. 1978. Quantum jumps of conductance during formation of membrane channels at cell-cell junction. *Nature (Lond.)* 274:133-136.
28. Lowry, O. H., N. J. Rosebrough, A. L. Farr, and R. J. Randall. 1951. Protein measurement with the Folin phenol reagent. *J. Biol. Chem.* 193:265-275.
29. Makowski, L., D. L. D. Caspar, W. C. Phillips, and D. A. Goodenough. 1977. Gap-junction structures. II. Analysis of the x-ray diffraction data. *J. Cell Biol.* 74:629-645.
30. Nicholson, B. J., M. W. Hunkapiller, L. E. Hood, and J. P. Revel. 1980. Partial sequencing of the gap junctional protein from rat lens and liver. *J. Cell Biol.* 87 (2, Pt. 2):200a (abstr.).
31. Ornstein, L. 1964. Disc electrophoresis. I. Background and Theory. *Ann. N. Y. Acad. Sci.* 121:321-349.
32. Rose, B., and W. R. Loewenstein. 1975. Permeability of cell junction depends on local cytoplasmic calcium activity. *Nature (Lond.)* 254:250-254.
33. Schuetze, S. M., and D. A. Goodenough. 1980. Developmental change in CO<sub>2</sub> sensitivity of chick lens intercellular coupling. *Society for Neuroscience Abstract.* 6:287.
34. Scornik, O. A., and V. Botbol. 1976. Role of changes in protein degradation in the growth of regenerative livers. *J. Biol. Chem.* 251:2891-2897.
35. Swick, R. W., and M. M. Ip. 1974. Measurement of protein turnover in rat liver with [<sup>14</sup>C]carbonate. *J. Biol. Chem.* 249:6386-6841.
36. Tanabe, T., W. Pricer, and G. Ashwell. 1979. Subcellular membrane topology and turnover of rat hepatic binding protein specific for asialoglycoproteins. *J. Biol. Chem.* 254:1038-1043.
37. Turin, L., and A. Warner. 1977. Carbon dioxide reversibly abolishes ionic communication between cells of early amphibian embryo. *Nature (Lond.)* 270:56-57.
38. Turin, L., and A. E. Warner. 1980. Intracellular pH in early *Xenopus* embryos: its effect on current flow between blastomeres. *J. Physiol. (Lond.)* 300:489-504.
39. Unwin, P. N. T., and G. Zampighi. 1980. Structure of the junction between communicating cells. *Nature (Lond.)* 283:545-549.
40. Wong, M. M., N. P. Robertson, and J. Horwitz. 1978. Heat induced aggregation of sodium dodecyl sulfate-solubilized main intrinsic polypeptide isolated from bovine lens plasma membrane. *Biochem. Biophys. Res. Commun.* 84:158-165.
41. Yancey, S. B., P. Dewees, and J. P. Revel. 1980. *In vivo* incorporation of [<sup>35</sup>S]methionine into gap junctional proteins. *J. Cell Biol.* 87 (2, Pt. 2): 212a (abstr.).
42. Zampighi, G., and J. D. Robertson. 1977. On macula communicans structure. *Biophys. J.* 17:31a.